Elastoresistive and elastocaloric anomalies at magnetic and electronic-nematic critical points

Alexander T. Hristov, Matthias S. Ikeda, Johanna C. Palmstrom, Philip Walmsley, and Ian R. Fisher

Phys. Rev. B **99**, 100101 — Published 11 March 2019

DOI: 10.1103/PhysRevB.99.100101

Elastoresistive and Elastocaloric Anomalies at Magnetic and Electronic-Nematic Critical Points

Alexander T. Hristov,[1,2,3,*] Matthias S. Ikeda,[1,2,4,*] Johanna C. Palmstrom,[1,2,4] Philip Walmsley,[1,5,4] and Ian R. Fisher[1,2,4]

[1] *Geballe Laboratory for Advanced Materials, Stanford University, Stanford, CA 94305*
[2] *Stanford Institute for Materials and Energy Science, SLAC National Accelerator Laboratory, 2575 Sand Hill Road, Menlo Park, California 94025, USA*
[3] *Department of Physics, Stanford University, Stanford, CA 94305*
[4] *Department of Applied Physics, Stanford University, Stanford, CA 94305*
[5] *Stanford Institute for Materials and Energy Science, SLAC National Accelerator Laboratory, 2575 Sand Hill Road, Menlo Park, California 94025*

(Dated: January 22, 2019)

Using $Ba(Fe_{0.975}Co_{0.025})_2As_2$ as an exemplar material exhibiting second order electronic-nematic and antiferromagnetic transitions, we present measurements that reveal anomalies in the elastoresistance ($\partial\rho_{ij}/\partial\varepsilon_{kl}$) and elastocaloric effect ($\partial T/\partial\varepsilon_{kl}$) at both phase transitions for induced strains ϵ_{kl} that do not share the symmetry of either order parameter. Both effects are understood to arise from the effect of strain on the transition temperatures; in the region close to the phase transitions this leads to (1) similarity between the strain and temperature derivatives of the resistivity and (2) similarity between the elastocaloric effect and the singular part of the specific heat. These mechanisms for elastoresistance and elastocaloric effect should be anticipated for any material in which mechanical deformation changes the transition temperature. Furthermore, these measurements provide evidence that the Fisher-Langer relation $\rho^{(c)} \propto U^{(c)}$ between the scattering from critical degrees of freedom and their energy-density, respectively, holds near each of the transitions in the material studied under varying strain as it does for varying temperature.

In metals, critical anomalies in the resistivity and specific heat detect symmetry breaking order and its critical fluctuations, regardless of the symmetry broken by the order parameter. Perhaps the best-known theory connecting resistivity and specific heat in a critical system originates from Fisher and Langer.[1] Their work relates the critical contributions to the resistivity $\rho^{(c)}$ and to the energy-density $U^{(c)}$ in a ferromagnet, where the (c) superscript indicates the additive contribution to a quantity from the critical degrees of freedom. According to this relation, the anomaly in the temperature derivative of the resistivity, $\frac{d\rho^{(c)}}{dT}$, is proportional to the critical contribution to the specific heat, $C_p^{(c)}$. Though this correspondence was initially anticipated only above the magnetic Curie temperature, T_c, subsequent work clarified conditions under which the relation holds both above and below T_c and in both ferromagnets and antiferromagnets,[2] and also applied the Fisher-Langer relation to nonmagnetic systems.[3] Here, we study the effect of strain, ε_{ij}, on the same quantities studied by Fisher and Langer, the resistivity and energy-density.[4]

Strain-based experimental techniques are being adopted across scattering,[5–7] transport[8–11] and NMR measurements.[12–14] Typically in materials such as $Ba(Fe_{0.975}Co_{0.025})_2As_2$, where there is a second order electronic-nematic transition,[8,15–17] antisymmetric strain of the same symmetry as the nematic order parameter has been applied.[8,9,18] Here, rather than using strain of the same symmetry as the nematic or Neél order parameters, we instead induce strain belonging to different irreducible representations from the order parameters. Crucially, in this strain environment the distinction between the symmetric and broken symmetry phases remains sharp in the presence of such strain, even as the critical temperatures, T_S and T_N, generically shift. Close to criticality, we experimentally determine proportionality between critcal anomalies in the elastocaloric coefficient and the specific heat, and between critical anomalies in the elastoresistance and in $\frac{d\rho}{dT}$. These correspondences arise naturally from the strain dependence of the transition temperatures. Furthermore, these measurements appear consistent with the Fisher-Langer relation, evincing a generalized correspondence,

$$C_p^{(c)} \propto \frac{\partial\rho^{(c)}}{\partial T} \propto \frac{dU^{(c)}}{d\varepsilon_{xx}} \propto \frac{d\rho^{(c)}}{d\varepsilon_{xx}}, \tag{1}$$

near each phase transition in $Ba(Fe_{0.975}Co_{0.025})_2As_2$. Equation (1) is the key result of this work, and it is demonstrated experimentally in Fig. 1, which shows the temperature dependences of these four separate experimentally obtained quantities.

$Ba(Fe_{0.975}Co_{0.025})_2As_2$ is an under-doped iron-pnictide with two continuous phase transitions upon cooling.[15–17] The first is an electronically-driven tetragonal-to-orthorhombic transition at $T_S \approx 99$ K caused by a nematic order parameter of B_{2g} symmetry.[8,19] The second is an antiferromagnetic transition at $T_N \approx 93$ K. Due to the presence of spin orbit coupling, the antiferromagnetic polarization is along the nematic easy axis,[14] so both transitions are of an Ising class. The qualitative behaviour of the data in Fig. 1 can be understood by considering that

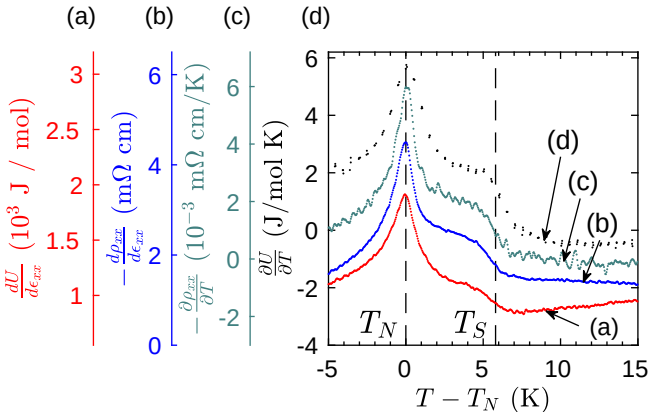

FIG. 1. (a-d) Temperature and strain derivatives of the resistance and energy in $Ba(Fe_{0.975}Co_{0.025})_2As_2$ in proximity to the successive nematic and Neél transitions, each plotted against a single corresponding axis on the left. Traces (a), (b), and (c) are obtained from a single sample with $T_N \approx 93$K. The specific heat shown in (d) is obtained from a second sample with $T_N \approx 92$K used in Ref. 16.

the antiferromagnetic phase transition is mediated by short range interactions for which the upper critical dimension $d_c^+ = 4$, whereas long range strain forces result in $d_c^+ = 2$ for the nematic transition.[20] Therefore, the overall structure of the traces in Fig. 1 reflects the fact that one transition occurs below and one transition occurs above the respective upper critical dimension, thus the anomalies consist of a pronounced peak at T_N and a mean-field-like step at T_S.[21]

The samples of $Ba(Fe_{0.975}Co_{0.025})_2As_2$ were grown by a self-flux method.[16] Reference specific heat data were obtained for a sample with $T_N \approx 92$ K and $T_S \approx 98$ K from Ref. 16, which used a standard relaxation technique in a Quantum Design Physical Property Measurement System. Measurements of resistivity, elastoresistivity, and elastocaloric effect were obtained simultaneously from a second sample ($T_N \approx 93$ K and $T_S \approx 99$ K), which has been measured previously to obtain precise values of the strain induced changes in the nematic and Neél transition temperatures.[11] The latter sample was cleaved to an approximate 0.035 mm c-axis thickness, then cut into a bar with axes oriented to those of the tetragonal unit cell, with approximate dimensions 2 mm $\times$ 0.4 mm.[11] Uniaxial stress was applied to the sample using a commercially available strain apparatus (CS100, Razorbill Instruments), which almost perfectly compensates the thermal expansion of $Ba(Fe_{0.975}Co_{0.025})_2As_2$ and allows the sample to be tuned near zero total strain at all temperatures.[11] The displacement-per-volt of the piezoelectric stacks was characterized by previous measurements[11] using an Andeen Hagerling AH2550A capacitance bridge; the displacement-per-volt of the PZT is frequency independent to a few percent.[22] The piezo devices were driven at frequencies from 1Hz to 30Hz, with a maximum amplitude of 7.5 V. Four-point electrical contact was made using Chipquik SMD291AX10T5 solder and gold wires. The voltage contacts were 0.65 mm apart, and the crystal was mounted with epoxy so that the middle portion the crystal, measuring 0.780 mm long and containing both voltage contacts, was between the mounting plates and experienced a piezo-driven mechanical deformation. The temperature derivative of the resistivity was obtained from a smoothing-spline fit to the raw resistivity data.

The elastoresistance of the sample was measured using an amplitude demodulation technique described previously,[22] using the dual-reference mode of a Stanford Research 860 lock-in amplifier. All elastoresistance signals so measured were frequency independent, indicating an intrinsic response not due to elastocaloric heating from the sample or strain device. The elastocaloric effect was measured by affixing a Type E chromel-constantan thermocouple onto the middle of the sample, where the strain is expected to be approximately uniform, using a thin layer of AngstromBond AB9110LV epoxy. The temperature oscillations at the strain frequency were measured with a lock-in technique.[23]

The application of a uniaxial stress σ_{xx} along the [100] axis induces a finite strain along all three crystal axes, as is evident by solving $\sum_{kl} c_{ijkl}\varepsilon_{kl} = \sigma_{ij}$, where c_{ijkl} is the elastic constant tensor and σ_{ij} is the stress. Following the framework presented by Ikeda *et al.*,[11] combination of strains can be written, using compact Voigt notation for the elastic constants, in a basis corresponding to irreducible representations of D_{4h}:

$$\varepsilon_{A_{1g},1} = \frac{1}{2}(\varepsilon_{xx} + \varepsilon_{yy}) = \frac{\sigma_{xx}}{2(c_{11} + c_{12} - 2\frac{(c_{13})^2}{c_{33}})} \quad (2)$$

$$\varepsilon_{A_{1g},2} = \varepsilon_{zz} = \frac{\sigma_{xx}}{2c_{13} - (c_{11} + c_{12})\frac{c_{33}}{c_{13}}} \quad (3)$$

$$\varepsilon_{B_{1g}} = \frac{1}{2}(\varepsilon_{xx} - \varepsilon_{yy}) = \frac{\sigma_{xx}}{2(c_{11} - c_{12})} \quad (4)$$

For the specific case of this sample and uniaxial stress along the [100] axis, the elastic constants in Eqs. (2) to (4) are only weakly temperature dependent and lack singular temperature dependence at criticality, so it is appropriate to approximate them as temperature-independent constants for a narrow range of temperatures in the vicinity of the critical temperatures. We emphasize, however, that this may not be appropriate (i) over a wider range of temperatures or (ii) for $Ba(Fe_{0.975}Co_{0.025})_2As_2$ samples under B_{2g} strain, where the shear modulus c_{66} softens due to coupling to order parameter fluctuations.[19]

The strains induced by uniaxial stress, shown in Eqs. (2) to (4), belong to irreducible representations of the D_{4h} point group which exclude the nematic and Neél order parameters. Strains such as these do not have bilinear coupling to either order parameter in the Landau free energy.[18] Instead, these strains influence the electronic order through free-energy terms that depend on

second order moments of each order parameter. Therefore, a primary effect of such strain is to vary the transition temperature T_i, which in $Ba(Fe_{0.975}Co_{0.025})_2As_2$ is either T_S for the nematic/structural transition or T_N for the Neél transition, according to

$$T_i = T_{i,0} - \Lambda^{(1)}_{\alpha,i}\varepsilon_\alpha - \Lambda^{(2)}_{\alpha,i}(\varepsilon_\alpha)^2 + \ldots, \qquad (5)$$

where ε_α is one of the strains in Eqs. (2) to (4). By symmetry, $\Lambda^{(1)}_{\alpha,i} \neq 0$ only for 'trivial' strains which break no additional crystal symmetries, such as ε_{zz} for a tetragonal material. However, the discussion phrased in terms of this general form (Eq. (5)) simultaneously applies both when α is trivial and non-trivial.[24] We noted earlier that for a sample aligned along the principal tetragonal axes, multiple strains are applied simultaneously and are all in approximately fixed proportion to each other and ε_{xx}. To treat multiple simultaneous strains of fixed proportion, we define $\nu^\alpha_{xx} = \varepsilon_\alpha/\varepsilon_{xx}$ for each irreducible representation and replace Eq. (5) by a sum over the α, which yields $\frac{dT_i}{d\varepsilon_{xx}} = \sum_\alpha \nu^\alpha_{xx}\Lambda^{(1)}_{\alpha,i}$ and $\frac{d^2T_i}{d\varepsilon^2_{xx}} = \sum_\alpha(\nu^\alpha_{xx})^2\Lambda^{(2)}_{\alpha,i}$. For $Ba(Fe_{0.975}Co_{0.025})_2As_2$, these coefficients have been reported in Ref. 11 for each of the two phase transitions; the linear response is $\frac{dT_N}{d\varepsilon_{xx}} = -629 \pm 2$ K, and $\frac{dT_S}{d\varepsilon_{xx}} = -521 \pm 4$ K. While there is no general (symmetry) reason for these two quantities to be within a factor of 2, it presumably reflects common electronic physics driving the magnetic and the structural transitions which remains as yet undeciphered in the pnictides. This greatly simplifies the following analysis, in that the strain-induced changes in T_N and T_S give rise to elastocaloric and elastoresistive anomalies of comparable magnitude at the two transitions.

The relation between the elastoresistivity and resistivity is shown in Fig. 2. Inspection reveals a close similarity between the temperature derivative of the resistivity $\partial\rho_{xx}/\partial T$ (blue symbols in Fig. 2 (a)) and the elastoresistivity $\partial\rho_{xx}/\partial\varepsilon_{xx}$ (red symbols in Fig. 2 (b)). Motivated by this observation, we scale $\partial\rho_{xx}/\partial T$ by the average value of the strain-induced change in transition temperature $\frac{d[\frac{1}{2}(T_S+T_N)]}{d\varepsilon_{xx}} = -575$ K and plot $\frac{\partial\rho_{xx}}{\partial T}\frac{d[\frac{1}{2}[T_S+T_N]}{d\varepsilon_{xx}}$ (blue crosses in Fig. 2 (b)) alongside $\frac{d\rho_{xx}}{d\varepsilon_{xx}}$. Scaled this way, the data lie almost on top of each other when a constant offset is included (grey line). This paper argues that this correspondence is not accidental, but rather a direct consequence of the strain dependence of the critical temperature for each of Neél and nematic order.

Our explanation begins with an almost trivial observation: if a measured property has a critical anomaly on approach to a critical temperature T_i and strain changes the critical temperature, then under a strain ε the anomaly appears at $T_i(\varepsilon)$ not $T_i(0)$. Building on this observation, we note the strain perturbations chosen for this work do not change the 3-d Ising universality class of each phase transition, so the functional forms of critical anomalies remain approximately the same in the presence of strain.[25] Therefore, rather than consider temperature

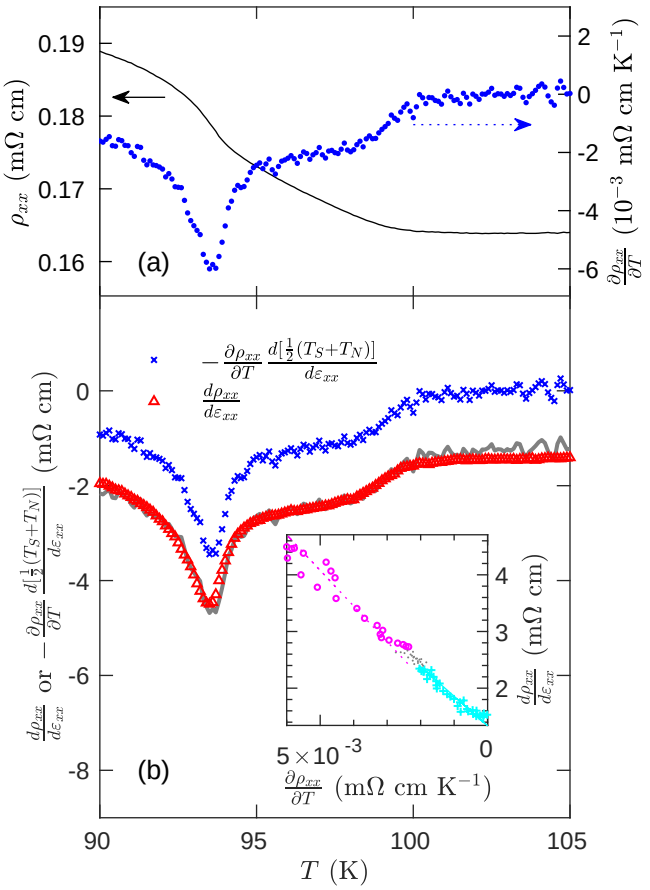

FIG. 2. (a) Resistivity of sample, plotted as a line against the left axis, and the temperature derivative shown against the right axis. (b) Comparison of $-\frac{\partial\rho}{\partial T}\frac{d[\frac{1}{2}(T_S+T_N)]}{d\varepsilon_{xx}}$ and $-\frac{d\rho_{xx}}{d\varepsilon_{xx}}$, motivated by discussion in the text. For the sake of comparison, the trace for $-\frac{\partial\rho}{\partial T}\frac{d[\frac{1}{2}(T_S+T_N)]}{d\varepsilon_{xx}}$ is reproduced with an offset of -1.24 mΩ cm as a solid gray line (behind the red data points). The inset shows the changes in $\frac{\partial\rho_{xx}}{\partial T}$ and $\frac{d\rho_{xx}}{\partial\varepsilon_{xx}}$. Cyan crosses represent temperatures in a window of ±2 K around the structural transition; magenta circles represent temperatures in a window of ±2 K around the Neél transition, and grey points represent temperates outside both windows. Straight lines show best fits using published values of $\frac{dT_N}{d\varepsilon_{xx}}$ (dashed magenta line) or $\frac{dT_S}{d\varepsilon_{xx}}$ (solid cyan line) over the corresponding temperature windows.[11]

and strain separately, we consider anomalous behavior in thermodynamic and transport properties as functions of $T - T_i(\varepsilon)$, where T_i represents T_S or T_N for each of the phase transitions.

The electronic scattering mechanisms are treated as independent and additive, so the diagonal components of the resistivity can be approximated as having a critical component $\rho^{(c)}$ and non-critical part $\rho^{(0)}$ satisfying

$$\rho_{xx}(T,\varepsilon_{xx}) \approx \rho^{(0)}_{xx}(T,\varepsilon_{xx}) + \rho^{(c)}_{xx}(T - T_i(\varepsilon_{xx})) \qquad (6)$$

for $i = S, N$ near each of the nematic and Neél transitions, respectively. This gives rise to an elastoresistive

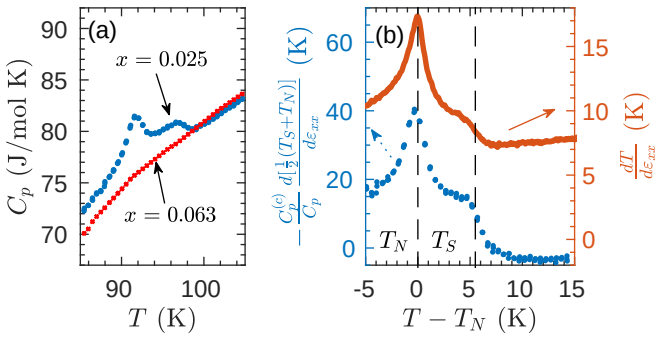

FIG. 3. (a) The specific heat of $Ba(Fe_{0.975}Co_{0.025})_2As_2$ from Ref. 16. The estimate of the heat capacity anomaly is obtained by subtracting the heat capacity of a sample of $Ba(Fe_{0.937}Co_{0.063})_2As_2$, which remains tetragonal and non-magnetic down to $T = 0$. (b) Arguments in the text lead to Eq. (9), according to which the critical part of elastocaloric effect (dashed line, right axis) should be exactly equal to the rescaled specific heat anomaly (dots, left axis). Both quantities show similar features at both T_S and T_N. However, as discussed in the text, an amplitude difference between these two traces emerges from experimental considerations of the strain apparatus.

effect

$$\frac{d\rho_{xx}^{(c)}}{d\varepsilon_{xx}} = -\frac{\partial\rho_{xx}^{(c)}}{\partial T}\frac{dT_i}{d\varepsilon_{xx}}. \tag{7}$$

If $\rho^{(0)}$ has a gradual temperature dependence, the above relation manifests in the derivatives of the total resistivity, as is evident in Fig. 2, and furthermore wherever the Fisher-Langer relation holds, it follows that this elastoresistive response tracks the specific heat. Motivated by Eq. (7), we plot in the inset to Fig. 2 $\frac{d\rho_{xx}}{d\varepsilon_{xx}}$ versus $\frac{\partial\rho_{xx}}{\partial T}$, and overlay linear best fits for the fixed proportionality constants of $\partial T_i/\partial\varepsilon_{xx}$ in the proximity of each phase transition. As can be seen the data are consistent with these estimates, up to systematic effects depending on the region around T_S and T_N where the fit is performed.

The same model can also be applied to measurements of the heat capacity and elastocaloric effect shown in Fig. 3. As before, the energy-density U is separated into a critical component $U^{(c)}$ and non-critical component $U^{(0)}$. As the stress is varied, the critical part of internal energy follows

$$\frac{dU^{(c)}}{d\varepsilon_{xx}} = -C_p^{(c,i)}\frac{dT_i}{d\varepsilon_{xx}}, \tag{8}$$

where $C_p^{(c,i)} = \frac{\partial U^{(c)}}{\partial T}$ is the anomaly in the specific heat at T_i and the total specific heat is C_p. Neglecting strain effects on the non-critical degrees of freedom and allowing critical degrees of freedom equilibrate with the other degrees of freedom, the leading contribution to the elastocaloric coefficient is

$$\frac{dT}{d\varepsilon_{xx}} = -\frac{C_p^{(c,i)}}{C_p}\frac{dT_i}{d\varepsilon_{xx}} + \ldots. \tag{9}$$

Figure 3 (a) shows the specific heat anomalies, $C_p^{(c,i)}$ of a sample of $Ba(Fe_{0.975}Co_{0.025})_2As_2$ obtained by Chu, *et al.* in Ref. 16 by subtracting a "background" contribution taken to be the measured specific heat of $Ba(Fe_{0.937}Co_{0.063})_2As_2$, for which both transitions are absent. Figure 3 (b) shows in the upper trace, plotted against the right axes, corresponding anomalies in the elastocaloric coefficient. There is a clear correspondence in both the shape of the peak at T_N and the mean-field-like step in both specific heat and elastocaloric coefficient right near T_S. Figure 3 (b) also shows the effect of scaling the specific heat anomaly according to Eq. (9) to predict the elastocaloric coefficient. The difference in magnitude between traces in Fig. 3 (b), approximately a factor of 5, can be quantitatively understood as the result of experimental limitations in the strain apparatus. Heat from the elastocaloric effect is generated solely by the strained portion of the sample,[26] but is dissipated throughout the whole sample and some way into the glue within the timescale of the measurement,[27] thus reducing the amplitude of the temperature modulation. In case the measurement is performed using high frequencies, or equivalently, oneshort time scales, the temperature sensors heat capacity becomes significant compared to the heat capacity of the fraction of the sample thermalizing to it. Most importantly, it should be noted that the observed elastocaloric effect in the sample cannot stem from self heating effects,[28] nor from any elastocaloric effect within the PZT stacks.[29] Furthermore, our detailed characterization of the experiment[23] shows that variation of the thermal properties of the sample and the glue together produce temperature dependence of the thermal transfer function less than 5 % for the strain frequency chosen and the temperature window under investigation. The temperature dependence of the elastocaloric effect signal thus purely reflects the thermodynamic signatures of the sample.

In conclusion, this work demonstrates elastocaloric and elastoresistive anomalies in $Ba(Fe_{0.975}Co_{0.025})_2As_2$ which track the specific heat and temperature derivative of the resistivity. Rather than using strain of the same symmetry as the order parameters, as has been used for measurements of thermodynamic suseptibilities,[8,9,18] these effects are realized by inducing strain belonging to different irreducible representations from the order parameter. The similarity of these four quantities, shown in Fig. 1, is consistent with a simple picture with just two rules for the critical parts of the resistivity and energy: they satisfy the Fisher-Langer relation and are functions of $T - T_i(\varepsilon)$ close to a phase transition at T_i.[30]

Finally, we note that even under circumstances in which the Fisher-Langer relation does not hold, and even for other types of order parameters than those studied here, 'isotropic' strain is a ubiquitous tuning parameter that always has a linear effect on the transition temperature. This results in (contributions to) an elastocaloric effect tracking the specific heat and an elastoresistivity tracking $\frac{d\rho}{dT}$, which may be useful for extracting $\frac{dT_i}{d\varepsilon}$ or

possibly the critical part of specific heat anomalies.[31] Furthermore, for other measurements like scattering or spin relaxation under strain, the strain dependence of the critical temperature can similarly admix the temperature derivative into measurements of the strain derivative unless forbidden by symmetry.

ACKNOWLEDGMENTS

We acknowledge helpful feedback on our ideas and the manuscript from S. A. Kivelson and T. Worasaran, and further acknowledge J.-H. Chu for providing the specific heat data originally published in Ref. 16. A.T.H. and J.C.P. are supported by a NSF Graduate Research Fellowship under grant DGE-114747. J.C.P. is also supported by a Gabilan Stanford Graduate Fellowship. M.S.I. and P.W. were partially supported by the Gordon and Betty Moore Foundations EPiQS Initiative through grant GBMF4414. This work was supported by the Department of Energy, Office of Basic Energy Sciences, under contract no. DE-AC02-76SF00515.

* These authors contributed equally to this work.
[1] M. E. Fisher and J. S. Langer, Phys. Rev. Lett. **20**, 665 (1968).
[2] S. Alexander, J. S. Helman, and I. Balberg, Phys. Rev. B **13**, 304 (1976).
[3] D. S. Simons and M. B. Salamon, Phys. Rev. Lett. **26**, 750 (1971).
[4] The strain derivative of the resistivity is measured directly, and the strain derivative of the energy-density is obtained from the product of the total specific heat (of which the critical contribution is less than 5 %) and the elastocalioric coefficient.
[5] X. Chen, L. Harriger, A. Sefat, R. J. Birgeneau, and S. D. Wilson, Phys. Rev. B **93**, 144118 (2016).
[6] C. Dhital, T. Hogan, Z. Yamani, R. J. Birgeneau, W. Tian, M. Matsuda, A. S. Sefat, Z. Wang, and S. D. Wilson, Phys. Rev. B **89**, 214404 (2014).
[7] D. W. Tam, Y. Song, H. Man, S. C. Cheung, Z. Yin, X. Lu, W. Wang, B. A. Frandsen, L. Liu, Z. Gong, T. U. Ito, Y. Cai, M. N. Wilson, S. Guo, K. Koshiishi, W. Tian, B. Hitti, A. Ivanov, Y. Zhao, J. W. Lynn, G. M. Luke, T. Berlijn, T. A. Maier, Y. J. Uemura, and P. Dai, Phys. Rev. B **95**, 060505 (2017).
[8] J.-H. Chu, H.-H. Kuo, J. G. Analytis, and I. R. Fisher, Science **337**, 710 (2012).
[9] H.-H. Kuo, M. C. Shapiro, S. C. Riggs, and I. R. Fisher, Phys. Rev. B **88**, 085113 (2013).
[10] C. W. Hicks, M. E. Barber, S. D. Edkins, D. O. Brodsky, and A. P. Mackenzie, Rev. Sci. Instrum. **85**, 065003 (2014).
[11] M. Ikeda, T. Worasaran, J. C. Palmstrom, P. Walmsley, and I. R. Fisher, "Symmetric and antisymmetric strain as continuous tuning parameters for electronic nematic order," (2018), arXiv:1803.09273.
[12] T. Kissikov, R. Sarkar, B. T. Bush, M. Lawson, P. C. Canfield, and N. J. Curro, Rev. Sci. Instrum. **88**, 103902 (2017).
[13] T. Kissikov, R. Sarkar, M. Lawson, B. T. Bush, E. I. Timmons, M. A. Tanatar, R. Prozorov, S. L. Bud'ko, P. C. Canfield, R. M. Fernandes, W. F. Goh, W. E. Pickett, and N. J. Curro, Phys. Rev. B **96**, 241108 (2017).
[14] T. Kissikov, R. Sarkar, M. Lawson, B. Bush, E. I. Timmons, M. A. Tanatar, R. Prozorov, S. Budko, P. C. Canfield, R. Fernandes, *et al.*, Nat. Commun. **9**, 1058 (2018).
[15] N. Ni, M. E. Tillman, J.-Q. Yan, A. Kracher, S. T. Hannahs, S. L. Bud'ko, and P. C. Canfield, Phys. Rev. B **78**, 214515 (2008).
[16] J.-H. Chu, J. G. Analytis, C. Kucharczyk, and I. R. Fisher, Phys. Rev. B **79**, 014506 (2009).
[17] C. Lester, J.-H. Chu, J. G. Analytis, S. C. Capelli, A. S. Erickson, C. L. Condron, M. F. Toney, I. R. Fisher, and S. M. Hayden, Phys. Rev. B **79**, 144523 (2009).
[18] The case of a transport measurement under an induced strain with the the same symmetry as the order parameter has been treated in M. C. Shapiro, P. Hlobil, A. T. Hristov, A. V. Maharaj, and I. R. Fisher, Phys. Rev. B **92**, 235147 (2015) and in the experiments referenced therein.
[19] R. M. Fernandes, A. E. Böhmer, C. Meingast, and J. Schmalian, Phys. Rev. Lett. **111**, 137001 (2013).
[20] U. Karahasanovic and J. Schmalian, Phys. Rev. B **93**, 064520 (2016).
[21] In both cases, the features are somewhat broadened, possibly reflecting the effect of quenched disorder or chemical inhomogeniety which can vary between crystals.
[22] A. T. Hristov, J. C. Palmstrom, J. A. W. Straquadine, T. A. Merz, H. Y. Hwang, and I. R. Fisher, Rev. Sci. Instrum. **89**, 103901 (2018).
[23] A manuscript explaining details of the measurement technique will be presented elsewhere.
[24] In the limit of infinitesimal strains, one therefore anticipates that the linear variation from the A_{1g} strains will dominate over the quadratic contributions.
[25] The strains induced in the material belong to either the A_{1g} or B_{1g} representations, which preserve the secondary mirror symmetries broken by the nematic order, and the translational symmetry broken by antiferromagnetic order.
[26] Based on finite element simulations in Ref. 11, it is estimated that effectively only 56 % of the sample is strained.
[27] The specific heat of the epoxy between the sample and the bottom mounting plates, which presumably is the part of the mounting epoxy that is heated the most by the EC effect in the sample, approximately equals the total sample heat capacity. The thermocouple adds about 2% to the total sample heat capacity.
[28] Self heating effects within the PZT actuators would cause a temperature oscillation at double the strain frequency.
[29] Elastocaloric effect within the PZT stacks might cause a roughly temperature independent background signal but can not create signatures corresponding to the thermodynamic properties of the sample under investigation. Furthermore, the background signal has been found to be negligible by separate temperature measurements on the cell body.

[30] For $Ba(Fe_{0.975}Co_{0.025})_2As_2$, $i = S$ for the nematic/structural phase transition and, and $i = N$ for the Neél transition.
[31] V. Pasler, P. Schweiss, C. Meingast, B. Obst, H. Wühl, A. I. Rykov, and S. Tajima, Phys. Rev. Lett. **81**, 1094 (1998).